https://doi.org/10.20965/jrm.2016.p0304

Paper:

Reduced-Order Observer Based Sliding Mode Control for a Quad-Rotor Helicopter

Reesa Akbar*,, Bambang Sumantri*,**, Hitoshi Katayama***, Shigenori Sano*, and Naoki Uchiyama***

*Department of Mechanical Engineering, Toyohashi University of Technology
1-1 Hibarigaoka, Tempaku, Toyohashi, Aichi 441-8580, Japan
E-mail: {sano@me., uchiyama@}tut.ac.jp
**Department of Electrical Engineering, Politeknik Elektronika Negeri Surabaya
Raya ITS, Keputih Sukolilo, Surabaya 60111, Indonesia
E-mail: {reesa, bambang}@pens.ac.id
***Department of Electrical and Electronic Engineering, Shizuoka University
3-5-1 Johoku, Naka-ku, Hamamatsu 432-8561, Japan
E-mail: thkatay@ipc.shizuoka.ac.jp

[Received August 28, 2015; accepted March 22, 2016]

The reduced-order observer design we present estimates the velocity states of a quadrotor helicopter, or quadcopter, based on sampled measurements of position and attitude states. This observer is based on the forward-differentiation Euler model. The observer is robust enough against observation noise that the gain of a closed-loop controller is high enough to improve control performance. A sliding-mode controller stabilizes and implements quadcopter tracking control effectively, as is verified experimentally when compared to a conventional backward-difference method.

Keywords: reduced-order observer, quad-rotor helicopter, sampler data system, sliding mode controller, tracking control

1. Introduction

Research on controller design for an unmanned aerial vehicle (UAV), specifically a quad-rotor helicopter, or quadcopter, has advanced progressively in the last decades [1–9]. A quadcopter, as a class of vertical takeoff/landing UAV, has many advantages over other types of UAV thanks to its compactness and simple, highly maneuverable mechanical structure.

Control performance depends much on the availability of information on quadcopter states, which are often difficult to measure using sensors alone [10]. Quadcopter displacement such as position and attitude is measured by visual sensors or global positioning systems (GPS), and velocity information must be generated numerically to obtain all such states of the quadcopter. An inertial measurement unit (IMU) is used to measure the quadcopter's linear acceleration and angular velocity, which must be integrated numerically to obtain all states. In this study, we consider the case in which an observer is designed and applied to obtain all quadcopter states to improve control performance, typified by using the backward-differentiation Euler method. A low-pass filter obtains velocity information from position measurement.

Shabayek et al. proposed a vision-based system for estimating a quadcopter's attitude [11]. Cabecinhas et al. proposed measuring helicopter position and attitude based on a visual sensor system and developed a vision-based system for estimating a helicopter's position [6, 12–15]. Zhang et al. proposed a full six degree-of-freedom (DOF) pose estimation for the helicopter based on a vision system [16–18]. IMU or gyro systems are typically used for stabilization. If not all states are available from sensors, an observer is a reasonable choice. Guisser and Medromi proposed a high-gain observer for estimating velocity states from measured coordinate positions and yaw angles [19], i.e., designed based on a continuous system and evaluated by simulation. Benallegue et al. designed a high-order sliding-mode observer to estimate unmeasurable states appearing in controller design [20]. Such an observer also estimates disturbance or noise effective in state measurements [21–24]. These methods are, however, designed based on helicopter dynamics as a continuous-time system.

In most practical applications, a control system is developed by using a digital computer as the discrete-time controller of a continuous-time system. System dynamics is generally modeled as nonlinear continuous-time systems. Designing a controller using a digital computer requires that we consider dynamics as a discrete-time system consisting of a sampler, i.e., analog-to-digital converter, and a zero-order holder, i.e., a digital-to-analog converter, also known as sampled-data systems [25]. Because obtaining the exact discrete-time model of a nonlinear system is difficult, it is often approximated in a simple manner by using the Euler model [26].

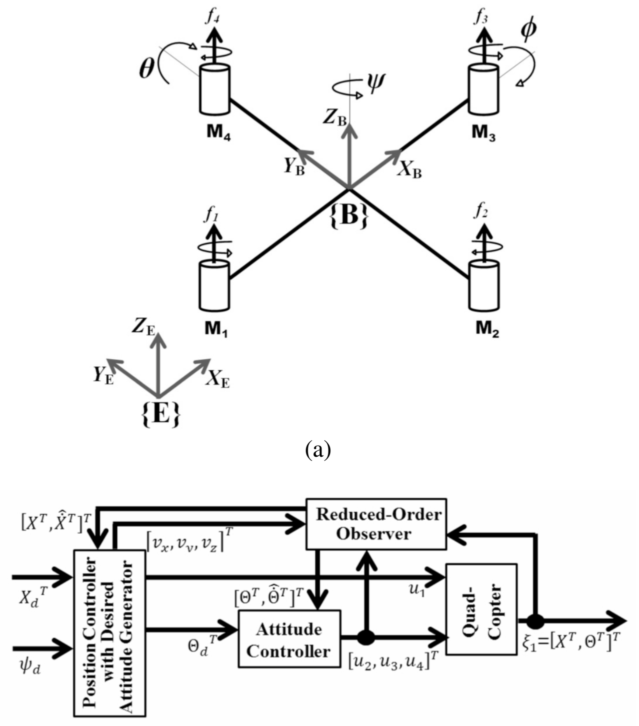

Fig. 1. (a) Coordinate system of quadcopter. (b) Control structure of quadcopter.

The reduced-order observer we designed is based on the Euler model of a quadcopter, including a practical, semiglobal discrete-time reduced-order observer [27] to estimate the velocity state assuming that position and attitude are available through sensors. We verified our method's effectiveness experimentally by using a sliding-mode controller (SMC). The SMC is applied in both translational and rotational motion control, giving us the advantages of the SMC as a robust controller in all DOF. We applied the least squares method to solve an over-determined control input problem in translational motion, for which reason we consider all six DOF in calculating control input.

Our main contribution in this work is to experimentally demonstrate the application of a discrete-time reduced-order observer [27] to a quadcopter together with its effectiveness. Sumantri et al. have proposed modeling dynamics and SMC controller design with full-state feedback [28, 29]. We extend their work to include the discrete-time reduced-order observer and to compare with the backward-difference method experimentally. We extend the SMC to an integral SMC to improve control performance.

2. Quadcopter Dynamics

Of a quadcopter's two pairs of contrarotating rotors, one pair rotates clockwise and the other counterclockwise as shown in **Fig. 1**. Lift for changing altitude is generated by rotating all rotors, yaw by accelerating the counterclockwise rotors and simultaneously decelerating the clockwise rotors, or vice versa. Forward motion is achieved by increasing rear rotor speed while simultaneously decreasing front rotor speed. Back, left and right motions are obtained similarly.

Quadcopter dynamics is modeled as a rigid 6-DOF body considering two frames – a body frame {B} fixed at the quadcopter's center of gravity and an earth-fixed frame {E}. The quadcopter's position and attitude are described with respect to frame {E} as shown in **Fig. 1(a)**, $X = [x, y, z]^T$ and $\Theta = [\phi, \theta, \psi]^T$.

Defining vectors $\dot{X}$ and $\dot{\Theta}$ as the quadcopter's linear and angular velocities in frame {E} and vectors v and ω as the linear and angular velocities in frame {B}, we get the following relation [28]:

$$\begin{aligned} \dot{X} &= Rv \\ \omega &= H\dot{\Theta}, \end{aligned}$$

where R and H are the rotation and translation matrix as follows:

$$R = \begin{bmatrix} -s\phi s\theta s\psi + c\theta c\psi & -c\phi s\psi & s\phi c\theta s\psi + s\theta c\psi \\ s\phi s\theta c\psi + c\theta s\psi & c\phi c\psi & -s\phi c\theta c\psi + s\theta s\psi \\ -c\phi s\theta & s\phi & c\phi c\theta \end{bmatrix}$$

$$H = \begin{bmatrix} c\theta & 0 & -c\psi s\theta \\ 0 & 1 & s\psi \\ s\theta & 0 & c\psi c\theta. \end{bmatrix}$$

Quadcopter dynamics is derived using Newton's equations of translational and rotational motion:

$$\ddot{\xi}_1 = f + U \quad \ldots\ldots\ldots\ldots\ldots \quad (1)$$

where

$$\begin{aligned} \xi_1 &= [X^T, \Theta^T]^T \\ f &= \begin{bmatrix} mI_{3\times3} & 0_{3\times3} \\ 0_{3\times3} & J \end{bmatrix}^{-1} [0, 0, -mg, K_1, K_2, K_3]^T, \\ U &= J \begin{bmatrix} mI_{3\times3} & 0_{3\times3} \\ 0_{3\times3} & J \end{bmatrix}^{-1} \begin{bmatrix} (s\phi c\theta s\psi + s\theta c\psi)u_1 \\ (-s\phi c\theta c\psi + s\theta s\psi)u_1 \\ c\phi c\theta u_1 \\ u_2 \\ u_3 \\ u_4 \end{bmatrix} \\ J &= \begin{bmatrix} I_x c\theta & 0 & -I_x c\phi s\theta \\ 0 & I_y & I_y s\phi \\ I_z s\theta & 0 & I_z c\phi c\theta \end{bmatrix} \\ K_1 &= (I_x + I_y - I_z)\dot{\phi}\dot{\theta}s\theta + (-I_x + I_y - I_z)\dot{\phi}\dot{\psi}s\phi s\theta \\ &\quad + (I_x + I_y - I_z)\dot{\theta}\dot{\psi}c\phi c\theta + (I_y - I_z)\dot{\psi}^2 s\phi c\phi c\theta, \\ K_2 &= (-I_y + (I_z - I_x)c2\theta)\dot{\phi}\dot{\psi}c\phi \\ &\quad + (I_z - I_x)\left(\dot{\phi}^2 - \dot{\psi}^2 c^2\phi\right)s\theta c\theta, \\ K_3 &= (-I_z + I_x - I_y)\dot{\phi}\dot{\theta}c\theta + (I_z + I_x - I_y)\dot{\phi}\dot{\psi}s\phi c\theta \\ &\quad + (I_z - I_x + I_y)\dot{\theta}\dot{\psi}c\phi s\theta - (I_x - I_y)\dot{\psi}^2 s\phi c\phi s\theta. \end{aligned}$$

Here, f is the aerodynamic force and moment vector, U is the control input vector. K_i, $i = 1, 2, 3$ is the moment of pitch, roll, and yaw and J is the inertia matrix. I_x, I_y, and I_z are the quadcopter's moment of inertia around the x, y, and z axes of frame $\{B\}$. m is total quadcopter mass, g is gravitational acceleration, $I_{3\times3}$ and $0_{3\times3}$ are 3×3 identity and 3×3 null matrices. Input $u_1 = f_1 + f_2 + f_3 + f_4$ is total thrust produced by the four rotors (**Fig. 1(a)**), $u_2 = L(f_4 - f_2)$ is the torque difference between the left and right rotors, $u_3 = L(f_1 - f_3)$ is the torque difference between the rear and front rotors, and $u_4 = d(f_4 + f_2 - f_1 - f_3)$ is the torque difference between clockwise rotors M_2 and M_4 and counterclockwise rotors M_1 and M_3. L is the distance of each rotor from the center of gravity and d is a scaling factor from force to moment. s denotes sine and c cosine.

To simplify controller design for a quadcopter categorized as an underactuated system in which the number of inputs is fewer than the number of DOF, we transform the quadcopter's original underactuated dynamics described in Eq. (1) into a decoupled system [28]. Given that synthetic input $v = f + U$, the decoupled system in Eq. (1) is written in the following simple linear form:

$$\begin{cases} \dot{\xi}_1 = \xi_2 \\ \dot{\xi}_2 = v \end{cases} \qquad (2)$$

where $\xi_1 = \xi = [x, y, z, \phi, \theta, \psi]$ and $\xi_2 = \dot{\xi}$, $v = [v_x, v_y, v_z, v_\phi, v_\theta, v_\psi]^T$ is a new controller-design input vector enabling us to consider a fully actuated system.

Given aerodynamics and gyroscopic effects together with wind effects as disturbance, we rewrite the quadcopter's decoupled dynamics as follows:

$$\begin{cases} \dot{\xi}_1 = \xi_2 \\ \dot{\xi}_2 = v + \rho_d \\ y_1(k) = \xi_1(k) \end{cases} \qquad (3)$$

ξ_1 is the position, ξ_2 the velocity, v the synthetic input, and ρ_d the disturbance vector.

Generating actual control input u_1, u_2, u_3, and u_4 from v is explained in Section 3.

3. Observer-Based Output Sliding-Mode Controller

3.1. Design

A stable sliding surface is determined in sliding-mode control design, then a robust control strategy designed to force the system onto the sliding surface. Controller stabilization and tracking based on a sliding-mode control strategy is designed for the dynamics in Eq. (3). The sliding-surface equation for the dynamics in Eq. (3) is designed as follows [30]:

$$s = \dot{\varepsilon} + \lambda \varepsilon. \qquad (4)$$

ε and $\dot{\varepsilon}$ are the tracking error of ξ_1 and ξ_2, positions and velocities, to desired trajectories $\xi_d = [x_d, y_d, z_d, \phi_d, \theta_d, \psi_d]^T$ and $\dot{\xi}_d = [\dot{x}_d, \dot{y}_d, \dot{z}_d, \dot{\phi}_d, \dot{\theta}_d, \dot{\psi}_d]^T$, $\lambda = \mathrm{diag}\{\lambda_i\}$, $i = 1, 2, \ldots, 6$, is a matrix with positive diagonal elements, and $s = 0$; $s = [s_1, s_2, \ldots, s_6]^T$ is a sliding surface.

To improve tracking performance, an integral part is added to Eq. (4) to yield the following sliding-surface equation [31]:

$$s = \dot{\varepsilon} + \lambda \varepsilon + \alpha \int_0^t \varepsilon(\tau)\mathrm{d}\tau. \qquad (5)$$

$\alpha = \mathrm{diag}\{\alpha_i\}$, $i = 1, 2, \ldots, 6$, is a matrix with positive diagonal elements.

The control objective here is to force the system into the sliding-mode $s = 0$. Once the system reaches the sliding surface, the controller maintains this sliding-mode condition, robustness is provided, and error tracking converges exponentially to zero.

Considering the sliding surface in Eq. (4), control system dynamics is written as follows:

$$\dot{s} = \ddot{\varepsilon} + \lambda \dot{\varepsilon}. \qquad (6)$$

Substituting $\ddot{\varepsilon} = \ddot{\xi}_d - \xi_2$ and Eq. (3) into Eq. (6) gives

$$\dot{s} = \ddot{\xi}_d - v - \rho_d + \lambda \dot{\varepsilon}. \qquad (7)$$

$\ddot{\xi}_d$ is the desired acceleration.

To achieve condition $s = 0$, we consider synthetic control input v with a constant plus proportional rate reaching law as follows:

$$v = \hat{u} + ks + q\,\mathrm{sign}(s). \qquad (8)$$

$k = \mathrm{diag}\{k_i\}$ and $q = \mathrm{diag}\{q_i\}$ are positive diagonal elements, and sign(.) is a signum function defined as follows:

$$\mathrm{sign}(s) = \begin{cases} 1 & \text{if } s > 0 \\ 0 & \text{if } s = 0 \\ -1 & \text{if } s < 0 \end{cases}$$

$\hat{u}$ is equivalent control input for dynamics in Eq. (7):

$$\hat{u} = \ddot{\xi}_d + \lambda \dot{\varepsilon}. \qquad (9)$$

Taking the integral sliding-surface equation in Eq (5) into consideration, equivalent control input is as follows:

$$\hat{u} = \ddot{\xi}_d + \lambda \dot{\varepsilon} + \alpha \varepsilon. \qquad (10)$$

$\alpha = \mathrm{diag}\{\alpha_i\}$.

The control strategy in Eq. (8) provides only the synthetic input υ, however, so to obtain original input u_1, u_2, u_3, and u_4, we use the method in [28]. Considering Eqs. (1) and (3) for rotational motion dynamics, we have

$$[u_2, u_3, u_4]^T = J[v_\phi, v_\theta, v_\psi]^T - [K_1, K_2, K_3]^T. \qquad (11)$$

Input u_1 is obtained from Eqs. (1) and (3) for translational motion dynamics by using the least squares method as follows [28]:

$$u_1 = m\sqrt{v_x^2 + v_y^2 + (v_z + g)^2}. \qquad (12)$$

3.2. Reduced-Order Observer

The quadcopter is a second-order nonlinear system having position and velocity states, as shown in Eq. (1). We assume only position states, i.e., absolute position and attitude, at each sampling time to be measurable. Velocity states are estimated by using a reduced-order observer [27] (see Appendix A). This reduced-order observer has the advantage of being applicable to nonlinear sampled-data systems, including the quadcopter. To implement a controller on a digital computer, sampled data must be handled appropriately, even though most observers consider only continuous or linear discrete systems.

We rewrite the quadcopter dynamics in Eq. (1) as follows in state space form:

$$\begin{cases} \dot{\xi}_1 = \xi_2 \\ \dot{\xi}_2 = f + U \\ y_1(k) = \xi_1(k) \end{cases} \qquad (13)$$

We consider the assumptions given in the Appendix A for applying the reduced-order observer:

A1: Mappings f_1, f_2, and g_1 in Eq. (20) are smooth over compact domain of interest, $f_1(0) = 0$, and $f_2(0,0,0) = 0$.

A2: $m \times m$ matrix $\Phi(\cdot) = g_1(\cdot)^T g_1(\cdot)$, where g_1 is defined as shown in Eq. (20), is nonsingular, and its inverse is bounded over the compact domain of interest.

Comparing Eqs. (13) and (20), we have $f_1(\xi_1) = 0$, $g_1(\xi_1) = 1$, $f_2(\xi_1,\xi_2,u) = f + U$. Because f in Eq. (13) includes the term mg, $f_2(\xi_1,\xi_2,u) = f + U$ does not satisfy assumption A1 if u is set to zero. We thus consider new control inputs v_x, v_y, and v_z in Eq. (2) as $u = [v_x, v_y, v_z, u_2, u_3, u_4]^T$ to cancel the term mg. We thus meet both assumptions A1 and A2 required to design the reduced-order observer as follows:

$$\hat{\xi}_2(k) = (I - TH)\hat{\xi}_2(k-1) + TN_T. \qquad (14)$$

$k = 0,1,2,\ldots,T$ is a sampling instant, I is a 6×6 identity matrix, and H is a 6×6 diagonal matrix as explained in Appendix A, and

$$N_T = H\Psi_T + f_2(y_1(k-1), \Psi_T, u(k-1)),$$
$$\Psi_T = \frac{y_1(k) - y_1(k-1)}{T}.$$

Observed state $\hat{\xi}_2(k)$ is used in the closed loop controller design in Eq. (8).

3.3. Closed-Loop Structure

We classify the quadcopter as an underactuated system because it has four independent inputs and 6 DOF. To simplify controller design, we design the quadcopter control structure as shown in **Fig. 1(b)** by modifying the control structure in [1, 28].

The control structure consists mainly of two controller blocks – a position controller with the desired attitude generator and an attitude controller. The position controller generates input u_1 by using the least squares method [28] and the desired attitude of the quadcopter, roll angle (ϕ_d) and pitch angle (θ_d), while ψ_d remains as assigned. The attitude controller handles attitude tracking control and generates inputs u_2, u_3, and u_4. These controllers use the velocity feedback provided by the observer.

As shown in **Fig. 1(b)**, desired outputs x_d, y_d, z_d, and ψ_d are assumed to be given, while ϕ_d and θ_d are generated by the position controller as shown below. From the translational dynamics in Eqs. (1) and (3), we obtain a synthetic input equation, giving us

$$\begin{cases} m(v_x \cos\psi + v_y \sin\psi) = \sin\theta u_1 \\ m(v_x \sin\psi - v_y \cos\psi) = \sin\phi\cos\theta u_1 \\ m(v_z + g) = \cos\phi\cos\theta u_1 \end{cases} \qquad (15)$$

Solving Eq. (15) for the attitude variables and replacing them with desired variables, we have

$$\begin{cases} \phi_d = \arctan\left(\dfrac{v_x \sin\psi_d - v_y \cos\psi_d}{v_z + g}\right) \\ \theta_d = \arctan\left(\dfrac{v_x \cos\psi_d + v_y \sin\psi_d}{\sqrt{(v_x \sin\psi_d - v_y \cos\psi_d)^2 + (v_z + g)^2}}\right) \end{cases} \qquad (16)$$

4. Experimental Results

We present experimental results to demonstrate the effectiveness of our proposed method using the quadcopter test bed shown in **Fig. 2(a)**. This test bed was built by attaching four rotors to rigid links for conducting the same experiments multiple times to verify repeatability. Potentiometers (S_1–S_5) measure all positions and attitudes. The experimental test bed parameters are as follows: $m = 0.285$ kg, $L = 0.212$ m, $g = 9.807$ m/s^2, $d = 1$ m, $I_x = I_y = 5.136 \times 10^{-3}$ kg.m^2, and $I_z = 1.016 \times 10^{-2}$ kg.m^2. The effectiveness of the reduced-order observer in Eq. (14) for estimating velocity is verified by comparing with the backward-difference method. To calculate velocity based on the backward-difference method, we applied a second-order low-pass filter with cut-off frequency $\omega = 15$ Hz to reduce high-frequency noise:

$$\hat{\xi}_2(k) = \alpha\left[\hat{\dot{\xi}}_1(k) + 2\hat{\dot{\xi}}_1(k-1) + \hat{\dot{\xi}}_1(k-2)\right] - 2\beta\hat{\xi}_2(k-1) - \gamma\hat{\xi}_2(k-2) \qquad (17)$$

$$\hat{\dot{\xi}}_1(k) = \frac{\xi_1(k) - \xi_1(k-1)}{T} \qquad (18)$$

$$\alpha = \frac{(T\omega)^2}{(T\omega - 2)}\beta,\ \beta = \frac{T\omega - 2}{T\omega + 2},\ \gamma = \beta^2. \qquad (19)$$

$\hat{\dot{\xi}}_1(k)$ is the velocity signal estimated by the backward difference method at the k-th sampling instant. We obtained $\hat{\xi}_2(k)$ by using the second-order low-pass filter and used it for control.

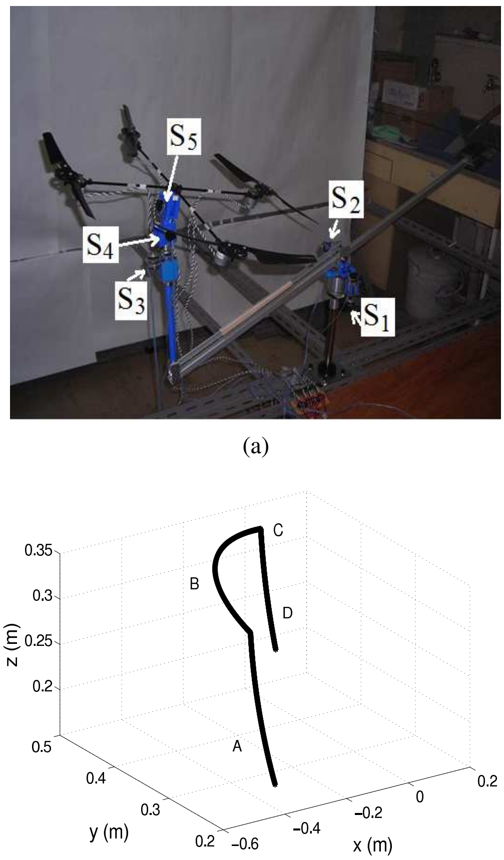

(a)

(b)

Fig. 2. (a) Quadcopter test bed. (b) 3D-desired trajectory.

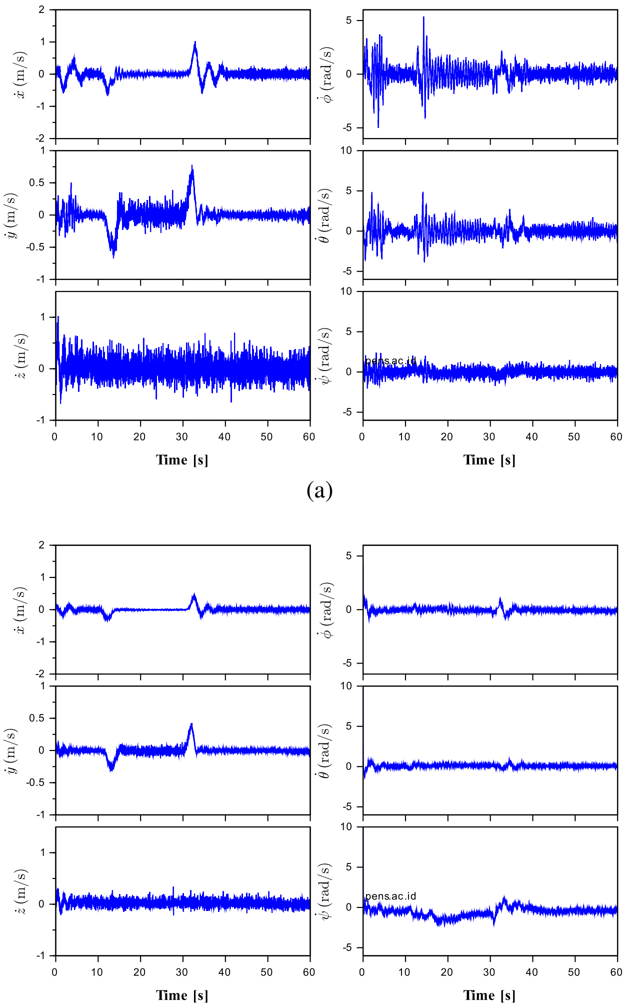

(a)

(b)

Fig. 3. Velocity profiles obtained by (a) the backward-difference method and (b) the reduced-order observer.

We used these estimated velocities in the SMC in Eq. (8), tuning control parameters for both methods to achieve the best experimental results, obtained as follows:

The SMC with a reduced-ordered observer is as follows:

$$k = \mathrm{diag}(6.5, 6, 16, 22, 20, 70),$$
$$\lambda = \mathrm{diag}(3, 4, 9, 8, 7, 40),$$
$$\lambda = \mathrm{diag}(90, 90, 100, 50, 60, 50),$$
$$q = \mathrm{diag}(0.6, 0.6, 1, 0.8, 0.8, 1),$$

The SMC with a backward-difference is as follows:

$$k = \mathrm{diag}(4, 3, 13, 11, 10, 30),$$
$$\lambda = \mathrm{diag}(3, 4, 9, 8, 7, 40),$$
$$q = \mathrm{diag}(0.6, 0.6, 1, 0.8, 0.8, 1),$$

The desired trajectory, shown in **Fig. 2(b)**, consists of the following four different motions within 60 s:

A: Take-off motion (0–10 s),

B: Maneuvering in the *x*-*y* plane (10–15 s),

C: Hovering by performing a yaw motion (15–45 s),

D: Landing (45–60 s).

Figures 3 and **4** show that the reduced-order observer reduces high-frequency signals more effectively than the backward-difference with a low-pass filter. Observer estimates reduce root mean square error (RMSE) by 37.4% and standard deviation of the velocity signal from the backward-difference method by 47.6% on the average. This observer estimates states relatively quickly, i.e., within 25 ms, corresponding to the fifth sampling time, which is useful from a real-time application point of view.

The reduced-order observer enables us to choose SMC gains relatively higher than those using the backward-difference method, improving tracking performance as shown in **Fig. 5**, which shows that the SMC using the reduced-order observer produces lower tracking error as shown in **Fig. 6**. The SMC with the sliding-surface function in Eq. (4), however, provides relatively higher tracking error. To improve tracking performance, we designed an integral sliding surface in Eq. (5). The experimental gain of the integral part is tuned and obtained as

$$\alpha = \mathrm{diag}\{0.5, 0.5, 0.6, 0.4, 0.2, 0.6\}.$$

The effectiveness of this sliding-surface design is shown in **Fig. 7**. The integral SMC reduces the RMSE

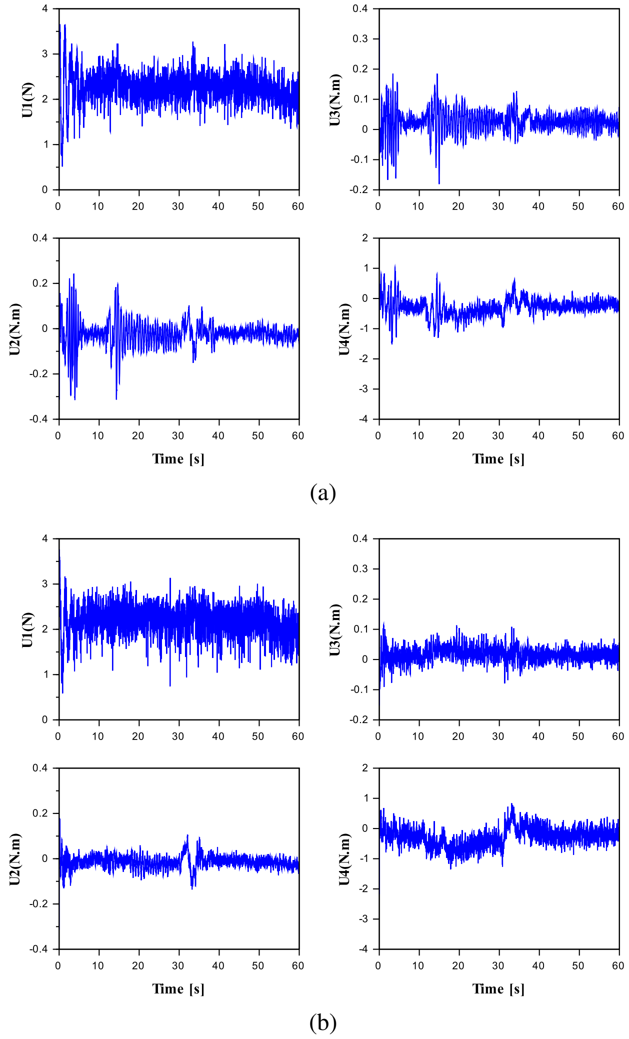

Fig. 4. Control input profiles by (a) the backward-difference method and (b) the reduced-order observer.

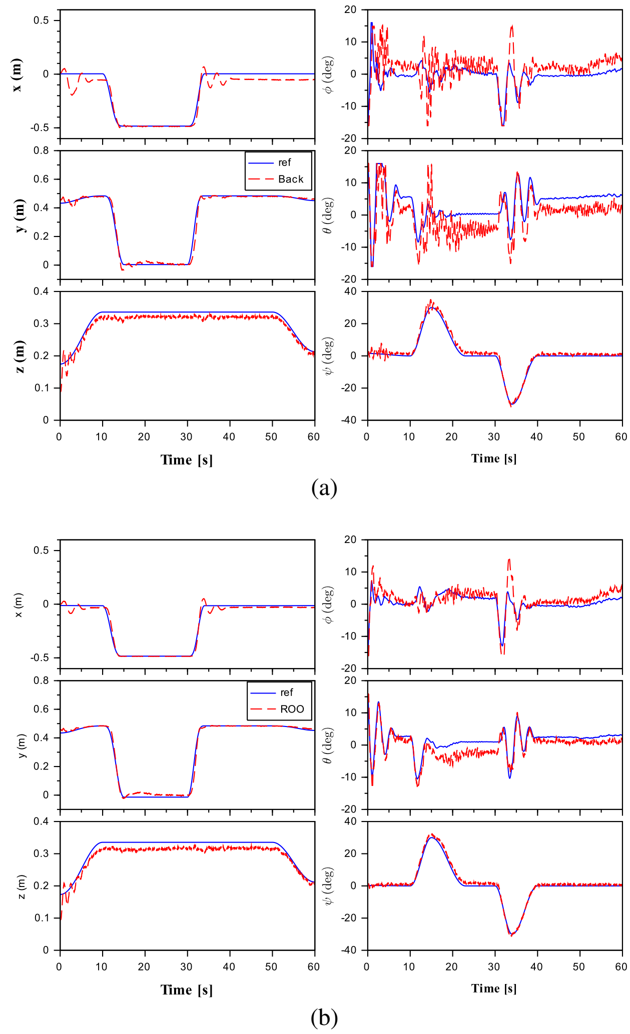

Fig. 5. Tracking control results by (a) the backward-difference method, Back, and (b) the reduced-order observer, ROO.

from the SMC by 10.9% on the average.

We verified the reliability of our proposed method by performing several experiments under the same condition. The RMSE and standard deviation for both methods are summarized in **Fig. 8**, which shows that the SMC with a reduced-order observer performed better than the backward-difference method. The SMC with the backward-difference method provides different results in each trial, yield the steady performance obtained by the reduced-order observer.

5. Conclusions

We have presented a quadcopter velocity estimator based on the sampled-data of position measurement and confirmed the estimator's effectiveness based on a reduced-order observer in experiments. We designed an SMC for stabilizing and tracking the desired trajectory. We have also compared results to those of a backward-difference method combined with a low-pass filter. In experiments, the reduced-order observer estimates quadcopter velocity from its initial value within 25 ms after the fifth sampling time, proving that it is useful in terms of practical application. The reduced-order observer enables us to choose relatively higher gain for the closed-loop controller, hence greatly reducing tracking error. The proposed method reduces the RMSE in tracking by 37.4% and standard deviation of velocity signal from the backward-difference method by 47.6% on the average. The integral SMC reduces the RMSE in tracking from the SMC by 10.9% on the average. We confirmed the reliability of our proposed method through multiple experiments. Our future work includes position and attitude observation from the acceleration and angular velocity signals typically obtained from the IMU.

References:

[1] A. Mokhtari and A. Benallegue, "Dynamic feedback controller of Euler angles and wind parameters estimation for a quadrotor unmanned aerial vehicle," IEEE-Int. Conf. on Robotics and Automation, pp. 2359-2366, 2004.

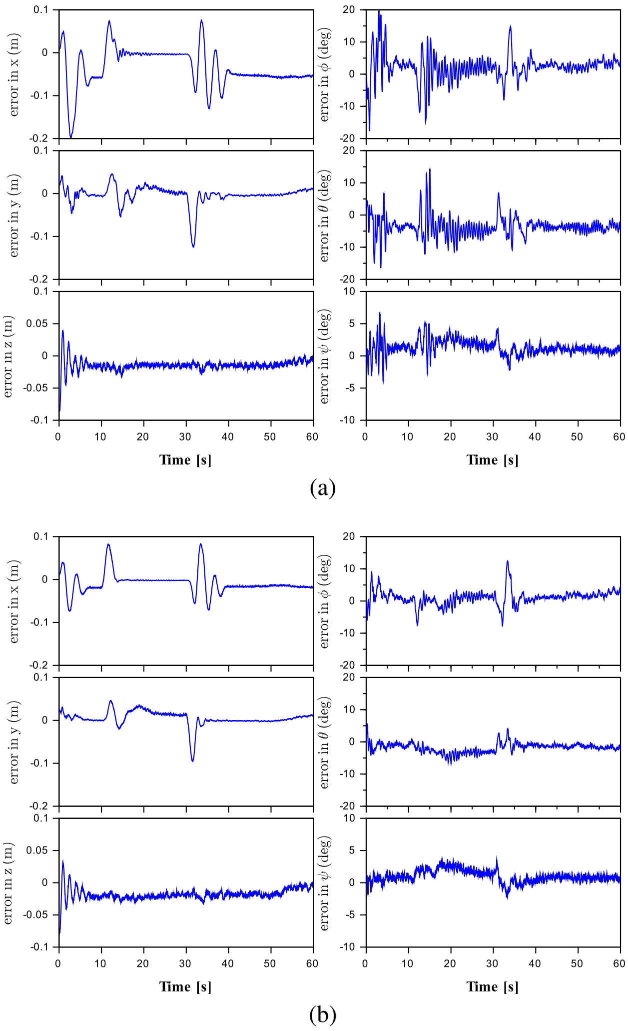

Fig. 6. Tracking error results by (a) the backward-difference method and (b) the reduced-order observer tracking control results.

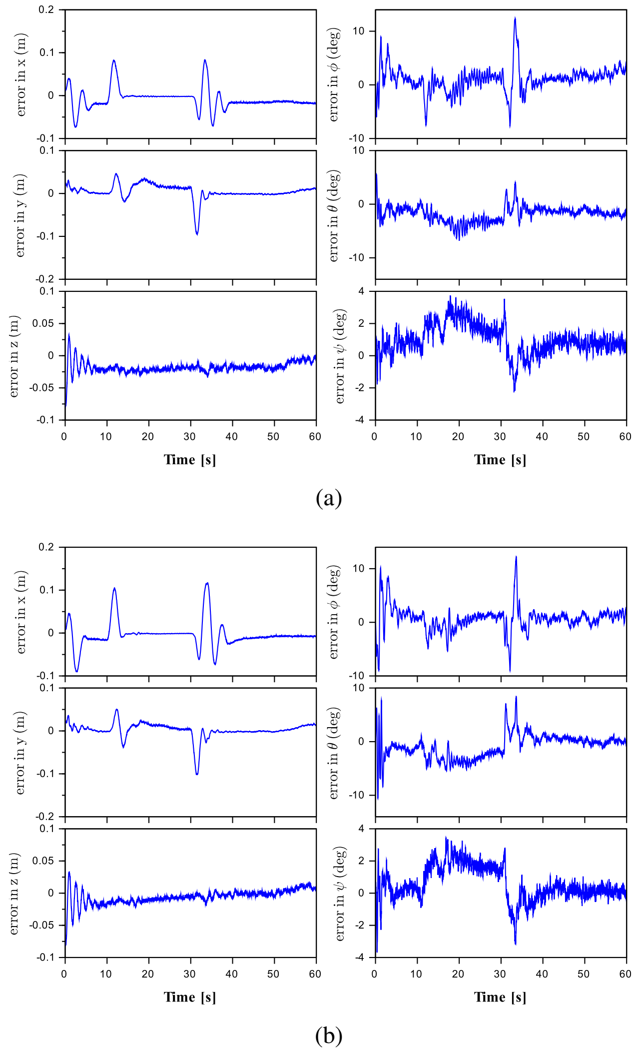

Fig. 7. Tracking error results by (a) SMC and (b) integral SMC.

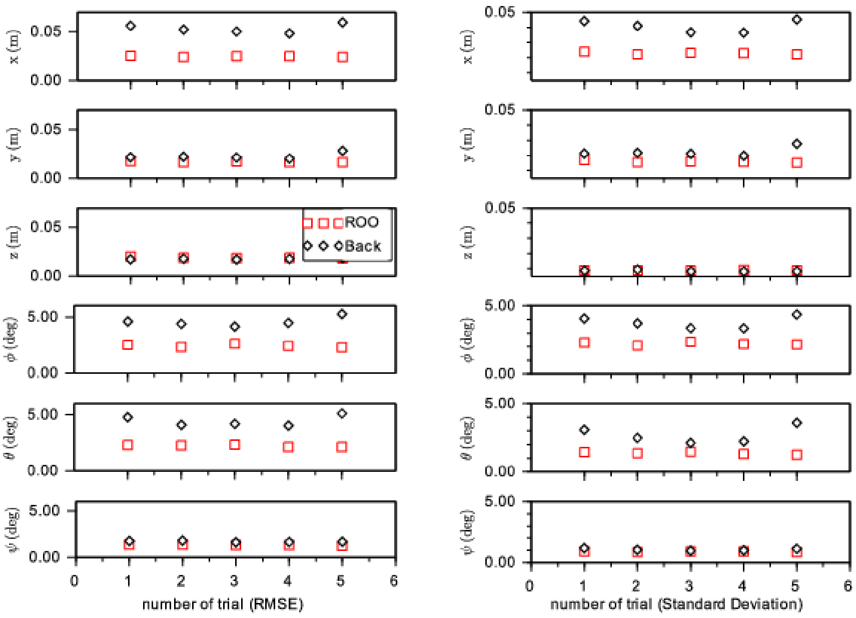

Fig. 8. RMSE and standard deviation with the reduced-order observer, ROO, and the backward-difference method, Back, from five experiments.

[2] M. Ichikawa, H. Yamada, and J. Takeuchi, "Flying Robot with Biologically Inspired Vision," J. of Robotics and Mechatronics, Vol.13, No.6, pp. 621-624, 2001.

[3] H. Nakanishi, H. Hashimoto, N. Hosokawa, K. Inoue, and A. Sato, "Autonomous Flight Control System for Intelligent Aero-robot for Disaster Prevention," J. of Robotics and Mechatronics, Vol.15, No.5, pp. 491-500, 2003.

[4] A. Mokhtari, A. Benallegue, and A. Belaidi, "Polynomial Linear Quadratic Gaussian and Sliding Mode Observer for a Quadrotor Unmanned Aerial Vehicle," J. of Robotics and Mechatronics, Vol.17, No.4, pp. 483-495, 2005.

[5] H. Nakanishi, S. Kanata, T. Sawaragi, and Y. Horiguchi, "Methods to Estimate Magnetic Declination for an Unmanned Aerial Vehicle," J. of Robotics and Mechatronics, Vol.20, No.4, pp. 541-549, 2008.

[6] D. Pebrianti, W. Wang, D. Iwakura, Y. Song, and K. Nonami, "Sliding Mode Controller for Stereo Vision Based Autonomous Flight of Quad-Rotor M," J. of Robotics and Mechatronics, Vol.23, No.1, pp. 137-148, 2011.

[7] M. F. B. Abas, D. Pebrianti, S. A. M. Ali, D. Iwakura, Y. Song, K. Nonami, and D. Fujiwara, "Circular Leader-Follower Formation Control of Quad-Rotor Aerial Vehicles," J. of Robotics and Mechatronics, Vol.25, No.1, pp. 60-71, 2013.

[8] D. Iwakura and K. Nonami, "Indoor Localization of Flying Robot by Means of Infrared Sensors," J. of Robotics and Mechatronics, Vol.25, No.1, pp. 201-210, 2013.

[9] R. M. Philbrick and M. B. Colton, "Effects of Haptic and 3D Audio Feedback on Operator Performance and Workload for Quadrotor UAVs in Indoor Environments," J. of Robotics and Mechatronics, Vol.26, No.5, pp. 580-591, 2014.

[10] V. Rejon and E. A. Bricaire, "Discrete-time dynamic feedback linearization of a VTOL using observed states," 17th IFAC-World Congress, Vol.17, pp. 1753-1759, 2008.

[11] A. R. Shabayek, C. Demonceaux, O. Morel, and D. Fofi, "Vision based UAV attitude estimation: progress and insights," Intelligent and Robotic Systems, Vol.65, pp. 295-308, 2011.

[12] S. Azrad, F. Kendoul, and K. Nonami, "Visual servoing of quadrotor micro-air vehicle using color-based tracking algorithm," System Design and Dynamics, Vol.4, No.2, pp. 255-268, 2010.

[13] D. Cabecinhas, S. Bras, C. Silvestre, P. Oliveira, and R. Cunha, "Integrated solution to quadrotor stabilization and attitude estimation using a pan and tilt camera," IEEE 51st Annual Conf. on Decision and Control, pp. 3151-3156, 2012.

[14] C. Schlaile, O. Meister, N. Frietsch, C. Kebler, J. Wendel, and G. F. Trommer, "Using natural features for vision based navigation of an indoor-VTOL MAV," Aerospace Science and Technology, Vol.13, pp. 349-357, 2009.

[15] Z. Yu, L. Tang, and K. Nonami, "Experiment in 3D vision based hovering control of an autonomous helicopter," System Design and Dynamics, Vol.1, No.4, pp. 660-671, 2007.

[16] M. Achtelik, T. Zhang, K. Kuhnlenz, and M. Buss, "Visual tracking and control of a quadcopter using a stereo camera system and inertial sensors," Int. Conf. on Mechatronics and Automation, pp. 2863-2869, 2009.

[17] E. Altug, J. P. Ostrowski, and C. J. Taylor, "Control of a quadrotor helicopter using dual camera visual feedback," Robotics Research, Vol.24, No.5, pp. 329-341, 2005.

[18] L. Zhang, T. Zhang, H. Wu, A. Borst, and K. Kuhnlenz, "Visual flight control of a quadrotor using bioinspired motion detector," Navigation and Observation, pp. 1-9, 2012.

[19] M. Guisser and H. Medromi, "A high gain observer and sliding mode controller for an autonomous quadrotor helicopter," Intelligent Control and Systems, Vol.14, No.3, pp. 204-212, 2009.

[20] A. Benallegue, A. Mokhtari, and L. Fridman, "High-order sliding-mode observer for a quadrotor UAV," Robust and Nonlinear Control, Vol.18, Issues 4-5, pp. 427-440, 2008.

[21] H. Bouadi and M. Tadjine, "Nonlinear observer design and sliding mode control of four rotors helicopter," Engineering and Applied Sciences, Vol.3, No.6, pp. 333-338, 2007.

[22] A. F. De Loza, H. Rios, and A. Rosales, "Robust regulation for a 3-DOF helicopter via sliding-mode observation and identification," Franklin Institute, Vol.349, pp. 700-718, 2012.

[23] A. Mokhtari, N. K. M'Sirdi, K. Meghriche, and A. Belaidi, "Feedback linearization and linear observer for a quadrotor unmanned aerial vehicle," Advanced Robotics, Vol.20, Issue 1, pp. 71-91, 2006.

[24] S. Suzuki, T. Ishii, N. Okada, K. Iizuka, and T. Kawamura, "Autonomous navigation, guidance and control of small electric helicopter," Int. J. of Advanced Robotic System, Vol.10, No.54, 2013.

[25] T. Chen and B. A. Francis, "Optimal Sampled-Data Control Systems," Springer, 1995.

[26] D. Nesic, A. R. Teel, and P. V. Kokotovic, "Sufficient conditions for stabilization of sampled-data nonlinear systems via discrete-time approximations," Systems and Control Letters, Vol.38, No.4, pp. 259-270, 1999.

[27] H. Katayama and H. Aoki, "Reduced-order observers for nonlinear sampled-data systems with application to marine systems," IEEE 52nd Annual Conf. on Decision and Control, pp. 5072-5077, 2013.

[28] B. Sumantri, N. Uchiyama, and S. Sano, "Least square based sliding mode control for a quad-rotor helicopter," IEEE/SICE Int. Symposium on System Integration, pp. 324-328, 2013.

[29] B. Sumantri, N. Uchiyama, and S. Sano, "Least square based sliding mode control for a quad-rotor helicopter and energy saving by chattering reduction," Mechanical Systems and Signal Processing, Vol.66-67, No.8, pp. 769-784, 2016.

[30] J. J. E. Slotine and W. Li, "Applied Nonlinear Control," Prentice Hall, 1991.

[31] K. Nonaka and H. Sugizaki, "Integral sliding mode altitude control for a small model helicopter with ground effect compensation," American Control Conf (ACC), pp. 202-207, 2011.

[32] H. K. Khalil, "Nonlinear Systems," Prentice Hall, 2002.

[33] H. Katayama and H. Aoki, "Straight-line trajectory tracking control for sampled-data underactuated ships," IEEE Trans. on Control Systems Technology, Vol.22, No.4, pp. 1638-1645, 2014.

Appendix A. Reduced-Order Observer Overview

Katayama and Aoki [27] considered a nonlinear sampled-data strict-feedback system in their work as follows:

$$\begin{cases} \dot{\zeta}_1 = f_1(\zeta_1) + g_1(\zeta_1)\zeta_2 \\ \dot{\zeta}_2 = f_2(\zeta_1, \zeta_2, u) \\ y_1(k) = \zeta_1(kT) \end{cases} \quad \ldots\ldots \quad (20)$$

$\zeta_1 \in \Re^{n_1}$ and $\zeta_2 \in \Re^{n_2}$ are continuous time states, $u \in \Re^m$ is control input realized through a zero order hold, $y_1 \in \Re^{n_1}$ is a sampled output from the sensor, and $T > 0$ is the sampling period. The system in Eq. (20) appears typically in the digital control of mechanical systems where ζ_1 and ζ_2 express the position and velocity, respectively, and $y_1(k) = \zeta_1(kT)$ means that only the position measurement at each sampling time is available for control. It also assumes the following:

A1: Mappings f_1, f_2, and g_1 are smooth over the compact domain of interest, $f_1(0) = 0$, and $f_2(0,0,0) = 0$.

A2: $m \times m$ matrix $\Phi(\cdot) = g_1(\cdot)^T g_1(\cdot)$ is nonsingular and its inverse is bounded over the compact domain of interest.

Let $u(t) = u(kT) =: u(k)$ for any $t \in [kT, (k+1)T)$. The difference equations corresponding to the exact model and the Euler approximate model of the system in Eq. (20) are then given by

$$\begin{cases} \eta_1(k+1) = \eta_1(k) + \\ \qquad \displaystyle\int_{kT}^{(k+1)T} [f_1(\eta_1(s)) + g_1(\eta_1(s))\eta_2(s)]\mathrm{d}s \\ \eta_2(k+1) = \eta_2(k) + \\ \qquad \displaystyle\int_{kT}^{(k+1)T} [f_2(\eta_1(s), \eta_2(s), u(k))]\mathrm{d}s \\ y_1(k) = \eta_1(k) \end{cases}$$

$$\ldots\ldots\ldots\ldots\ldots\ldots \quad (21)$$

and

$$\begin{cases} \eta_1(k+1) = \eta_1(k) + T[f_1(\eta_1(k)) + g_1(\eta_1(k))\eta_2(k)] \\ \eta_2(k+1) = \eta_2(k) + T[f_2(\eta_1(k), \eta_2(k), u(k))] \\ \quad y_1(k) = \eta_1(k), \end{cases} \quad (22)$$

Note that $(\zeta_1, \zeta_2)(kT) = (\eta_1, \eta_2)(k)$ for the exact model. The exact model is not generally computable, so we use the Euler approximate model for design. Then following equation

$$\begin{aligned} \hat{\eta}_2(k+1) = {} & (I - TH)\hat{\eta}_2(k) \\ & + TN_T(y_1(k), \rho y_1(k), u(k)) \end{aligned} \quad (23)$$

becomes the reduced-order observer of the Euler model in Eq. (22), where $H = \mathrm{diag}\{h_1, \dots, h_{n_2}\}$, $|1 - Th_i| < 1$, $i = 1, \dots, n_2$, ρ denotes the shift operator,

$$\begin{aligned} (\rho y_1)(k) &= y_1(k+1) \\ N_T(y_1, \rho y_1, u) &= H\Psi_T(y_1, \rho y_1) + f_2(y_1, \Psi_T(y_1, \rho y_1), u) \\ \Psi_T(y_1, \rho y_1) &= \Phi(y_1)^{-1} g_1(y_1)^T \cdot \\ & \quad \left\{ \frac{\rho y_1 - y_1}{T} - f_1(y_1) \right\}. \end{aligned}$$

This observer is semiglobal and practical in T for the exact model in Eq. (21), i.e., there exist $\beta \in \mathcal{KL}$ such that for any $D > d > 0$ and compact sets $\Omega_1 \in \Re^{n_1}$, $\Omega_2 \in \Re^{n_2}$, $U \in \Re^m$ we find $T^* > 0$ with the property that $||\eta_2(0) - \hat{\eta}_2(0)|| \leq D$ and $\eta_1(k) \in \Omega_1$, $\eta_2(k) \in \Omega_2$, and $u(k) \in U$ for any $k \geq 0$ imply $||\eta_2(k) - \hat{\eta}_2(k)|| \leq \beta(||\eta_2(0) - \hat{\eta}_2(0)||, kT) + d$ for all $T \in (0, T^*)$ [27], where $\beta \in \mathcal{KL}$ means that for any fixed $t \geq 0$, function $\beta(\cdot, t)$ is continuous, zero at zero, strictly increasing, and for each fixed $s \geq 0$, $\beta(s, \cdot)$ is decreasing to zero as its argument tends to infinity [32]. The robustness of the observer in Eq. (23) against sampled observation noise is discussed in [33].

Name:
Reesa Akbar

Affiliation:
Politeknik Elektronika Negeri Surabaya
Toyohashi University of Technology

Address:
Raya ITS, Keputih Sukolilo, Surabaya 60111, Indonesia
1-1 Hibarigaoka, Tempaku, Toyohashi, Aichi 441-8580, Japan

Brief Biographical History:
2001- Joined Politeknik Elektronika Negeri Surabaya (PENS)
2002- Administrator, Sun Microsystem Laboratory, PENS
2005- Member of Sensor Network Laboratory, PENS

Membership in Academic Societies:
• Indonesian Soft-Computing Forum

Name:
Bambang Sumantri

Affiliation:
Politeknik Elektronika Negeri Surabaya

Address:
Raya ITS, Keputih Sukolilo, Surabaya 60111, Indonesia

Brief Biographical History:
2002 Received B.E. from Institute of Technology of Sepuluh Nopember (ITS), Indonesia
2009 Received M.Sc. from Universiti Teknologi Petronas
2015 Received Dr.Eng. from Toyohashi University of Technology

Main Works:
• “Least square based sliding mode control for a quad-rotor helicopter and energy saving by chattering reduction,” Mechanical Systems and Signal Processing, Vol.66, pp. 769-784, 2016.

Name:
Hitoshi Katayama

Affiliation:
Associate Professor, Shizuoka University

Address:
3-5-1 Johoku, Naka-ku, Hamamatsu 432-8561, Japan

Brief Biographical History:
1994-2001 Lecturer, Faculty of Engineering, Osaka Electro-Communication University
2001- Associate Professor, Faculty of Engineering, Shizuoka University

Main Works:
• “Straight-line Trajectory Tracking Control for Sampled-data Underactuated Ships,” IEEE Trans. on Control Systems Technology, Vol.22, No.4, pp. 1638-1645, 2014.

Membership in Academic Societies:
• The Institute of Electrical and Electronics Engineers (IEEE)
• The Society of Instrument and Control Engineers (SICE)

Name:
Shigenori Sano

Affiliation:
Associate Professor, Toyohashi University of Technology

Address:
1-1 Hibarigaoka, Tempaku, Toyohashi, Aichi 441-8580, Japan

Brief Biographical History:

1999- Research Scientist, Bio-Mimetic Control Research Center, RIKEN
2001- Assistant Professor, Toyohashi University of Technology

Main Works:

- "LMI Approach to Robust Control of Rotary Cranes under Load Sway Frequency Variance," J. of System Design and Dynamics, Vol.5, No.7 pp. 1402-1417, 2011.

Membership in Academic Societies:

- The Japan Society of Mechanical Engineers (JSME)
- The Society of Instrument and Control Engineers (SICE)
- The Robotics Society of Japan (RSJ)

Name:
Naoki Uchiyama

Affiliation:
Professor, Toyohashi University of Technology

Address:
1-1 Hibarigaoka, Tempaku, Toyohashi, Aichi 441-8580, Japan

Brief Biographical History:

1995- Research Associate, Toyohashi University of Technology
2001-2002 Visiting Scholar, University of California, Davis

Main Works:

- "Energy Saving in Five-Axis Machine Tools Using Synchronous and Contouring Control and Verification by Machining Experiment," IEEE Trans. on Industrial Electronics, Vol.62, No.9, pp. 5608-5618, 2015.

Membership in Academic Societies:

- The Japan Society of Mechanical Engineers (JSME)
- The Japan Society for Precision Engineering (JSPE)
- The Society of Instrument and Control Engineers (SICE)
- The Institute of Systems, Control and Information Engineers (ISCIE)
- The Robotics Society of Japan (RSJ)
- Society of Automotive Engineers of Japan (JSAE)
- The Institute of Electrical and Electronics Engineers (IEEE)